On Improvement of Erosion Resistance of Titanium Parts Fabricated by 3D Printing Using DLC Coating

A.F. Mednikov, A.B. Tkhabisimov, S.V. Sidorov, O.S. Zilova, A.A. Burmistrov

Abstract: ***This article discusses experimental studies of resistance against water droplet impact erosion of Ti–6Al–4V samples fabricated by 3D printing without and with protecting DLC (Diamond–Like–Carbon) coating produced by magnetron sputtering. Erosion tests have been carried out using unique test facilities: Erosion–M hydroimpact test rig, Moscow Power Engineering Institute, at impingement velocity of C_{imp} = 300 m/s with monodisperse flow of liquid and droplet diameter of d_{dr} = 800 µm. The data on properties of DLC coating (elemental composition, thickness, microhardness) are given, the coatings have been formed on field samples: erosion resistant couplings made by 3D printing and simulating leading edge at periphery of rotating blades of the last stage of high-power steam turbine. The experimental and metallographic studies revealed efficiency of ion plasma DLC coatings, their application at the stage of incubation period would improve the erosion resistance of Ti–6Al–4V titanium alloy obtained using additive process by at least 1.4 times. On the basis of the obtained data, possibility of integrated application of 3D printing for fabrication of replaceable erosion resistant couplings with protecting coating on rotating blade periphery has been considered as an alternative to stellite plates widely applied as passive protection against water droplet impact erosion.***

Index Terms: ***3D printing, DLC coating, experimental studies, metallography, replaceable couplings, rotating blades, steam turbine, water droplet impact erosion.***

I. INTRODUCTION

Wide opportunities of additive technologies as an alternative to conventional fabrication of workpieces are applied in various industries, such as construction, automobile and spacecraft manufacturing, power generation, and others [1]–[3]. Their usage makes it possible to solve production tasks related with fabrication of shaped workpieces, with the use of high amount of material which is subsequently removed, as well as with the time consumption.

Nowadays it has been proven that the properties of metal workpieces fabricated by 3D printers, such as density, residual strains, mechanical behavior, nonequilibrium microstructure, crystallographic texture, are superior in comparison with those fabricated by casting, deformation or mechanical processing [4]–[8]. For instance, the strength of items produced by selective laser sintering is higher than those of casted ones by 2–12 % [9]. The strength of such workpieces is stimulated by small size of grains and microstructural components [10], [11]. On the basis of this, it is possible to control the properties of items in wide range. For instance, while applying such methods as variation of temperature conditions of solidification, alloying, addition of modifiers, thermal cycling, and others, it is possible to significantly improve strength of metals and alloys [12], [13].Our previous studies [14] have demonstrated that 3D printed workpieces, similar to those fabricated by conventional methods, are characterized by similar (nearly identical) resistance against droplet impingement erosion [15], which subsequently can be applied for fabrication of rotating blades of last stages of steam turbines. An urgent task appears in this regard related with development of integrated methods of improvement of erosion resistance of functional surfaces by combined application of various innovation engineering approaches which are possible due to improved efficiency of their fabrication by 3D printing and new promising compositions of wear resistant ion plasma coatings. Application of coatings is characterized by numerous advantages [16]–[19] in comparison with other protections of rotating blades. For instance, overall surface of rotating blade is protected and not only leading edges at periphery as upon protection by welding of stellite plates or by electrical discharge strengthening. Coating can be a universal tool to control both erosion and corrosion protecting overall blade surface during turbine operation and during standby of all equipment. The most promising ion plasma coatings are based on carbide nitrides and nitrides of titanium and chromium [16], [17] as well as wear resistant diamond-like-carbon (DLC) coatings. The DLC coating is amorphous coating comprised of combination of carbon with sp^2 and sp^3 hybridization (Fig. 1). Carbon with sp^2 hybridization is graphite, and sp^3 hybridization is characteristic for diamond. Therefore, DLC coating is nanocomposite coating with solid inclusions of carbon of sp^3 hybridization in amorphous matrix of carbon of sp^2 hybridization, which makes it possible to provide both elasticity and high microhardness of coating. Coating microhardness increases with the increase in amount of carbon phase of sp^3 hybridization, however, internal stresses in the coating also increase and its elasticity deteriorates [20]–[29].

Revised Manuscript Received on May 06, 2019

A.F. Mednikov, National research university «MPEI», Moscow, Russia.
A.B. Tkhabisimov, National research university «MPEI», Moscow, Russia.
S.V. Sidorov, National research university «MPEI», Moscow, Russia.
O.S. Zilova, National research university «MPEI», Moscow, Russia.
A.A. Burmistrov, National research university «MPEI», Moscow, Russia.

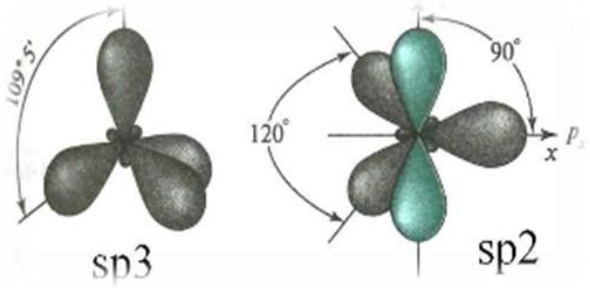

Fig. 1. Carbon hybridization phases: sp^3 and sp^2 [22]

In addition to carbon, in order to achieve certain properties, DLC coating can also contain carbide forming materials, such as silicon, titanium, chromium, hydrogen [23]. Preliminary experimental studies of erosion resistance of titanium samples fabricated by 3D printing with various protective coatings based on chromium and DLC coatings revealed the composition of coating the most resistant against pulse impact of liquid particles. According to the experimental results the DLC coating is the best, it improves erosion resistance of printed Ti–6Al–4V samples by 1.4÷1.6 times in terms of incubation period of erosion wear.

In addition to application of ion plasma coating as the main surface protection of rotating blades against high speed droplet impingement, an integrated approach to passive protection is known comprised of the use of detachable couplings fabricated of erosion resistant materials, including those with coatings. Various Western companies applied couplings, which is described in [6], [7].

The authors developed and proposed integrated approach to apply passive protection at periphery of rotating blade airfoil of the last stage of steam turbine in the form of erosion resistant replaceable couplings (Fig. 2) fabricated by 3D printing and subsequently strengthened by formation of protective coating. In this work 3D printing was used for fabrication of increased peripheral part of rotating blade, experimental samples (simulating leading edge and a part of coupling) aimed at analysis of erosion resistance and properties of DLC coating formed on the fabricated workpieces, as well as for testing the possibility to apply the proposed approach on full scale items.

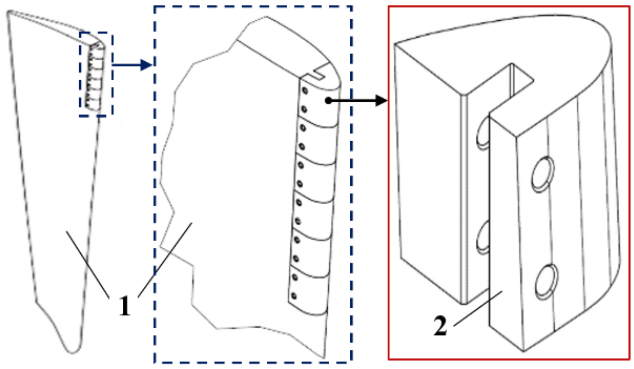

Fig. 2. Schematic view of the proposed approach to application of erosion resistant coupling with coating at rotating blade periphery: 1 – blade periphery, 2 – erosion resistant coupling with coating.

II. PROPOSED METHODOLOGY

A. Fabrication of Parts

Workpieces required for the studies were fabricated by 3D printing using a M2 Cusing laser printer (Fig. 3a). This brand is used for solution of various tasks in such industries as spacecraft, defense, food production, medicine and others [2].

Concept Laser M2 Cusing 3D printer operation is based on selective laser melting (SLM) [4] (Fig. 3b). Material used for fabrication of workpieces is applied with preset thickness (from 20 to 80 μm), then the melting follows according to CAD data for specified layer. Laser processing takes place in area with controllable environment. An important operation aspect of 3D printer is automated system of powder supply which increases the process rate and eliminates involvement of an operator for material feeding.

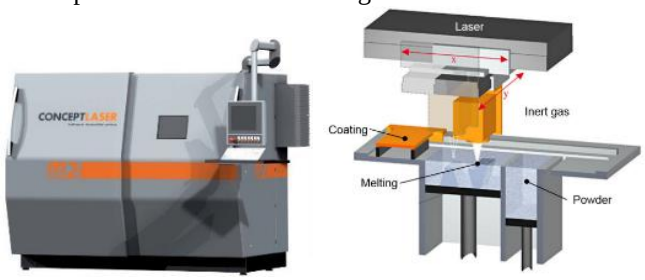

a) b)

Fig. 3. External view (a) and operation principle (b) of Concept Laser M2 Cusing 3D printer [30], [31].

The printed workpieces (erosion resistant couplings and peripheral parts of rotating blades) are illustrated in Fig. 4a. Because of design features of Erosion–M test rig [20], it is possible to perform tests only with special samples with preset root design [14]. Therefore, in order to perform erosion tests, samples were fabricated in the form of «mushrooms» with working part (Fig. 4b) of the same geometry as that of erosion resistant replaceable coupling.

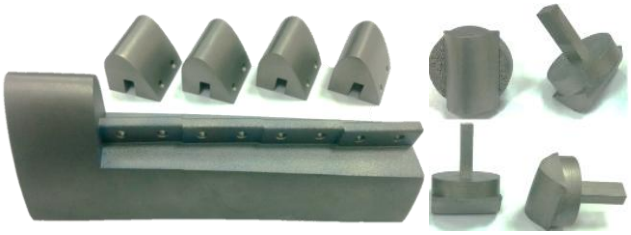

a) b)

Fig. 4. Parts (a) and special samples for erosion tests (b) fabricated by 3D printing

The workpieces and samples were fabricated of powdered Ti–6Al–4V. It was comprised of spherical particles with the sizes of 40–60 μm. Chemical composition of the material is summarized in Table I.

Table I. Chemical composition of Ti–6Al–4V powder

Element	Comp., %
Ti	Base
Al	5.9
Mo	–
V	4.1
Zr	0.07
Fe	0.2
N	0.03
C	0.07
H	0.01
O	0.1
Si	0.04
Impurities	< 0.3

III. FORMATION OF COATING

DLC based coating was formed using Gefest–HiPIMS facility, Moscow Power Engineering Institute (Fig. 5a). Experimental samples and workpieces were placed into vacuum chamber. Specially designed auxiliaries provided planetary rotation inside the facility (Fig. 5b). DLC coating was formed as follows. Preliminary fabricated workpieces and samples were placed into vacuum chamber, then the chamber was evacuated and the items were heated. After reaching the pressure of 10^{-4} Pa in the chamber, the preheating of workpieces and samples was deactivated, the vacuum valve was restricted by one half, and plasma forming gaseous argon was filled up to the pressure of 0.3 Pa. Negative voltage (bias voltage) of about 1,000 V was supplied onto the items moving planetary inside the vacuum chamber, glow discharge was initiated, and ionic cleaning was performed. After the ionic cleaning, the surface of workpieces and samples was coated with adhesive layer of pure carbide forming metal: titanium (*Ti*). After formation of adhesive layer, the intermediate layer of titanium carbide (*TiC*) was applied. Then the final coating layer was applied: *DLC*. The samples and erosion resistant couplings with formed DLC coating are illustrated in Fig. 5c.

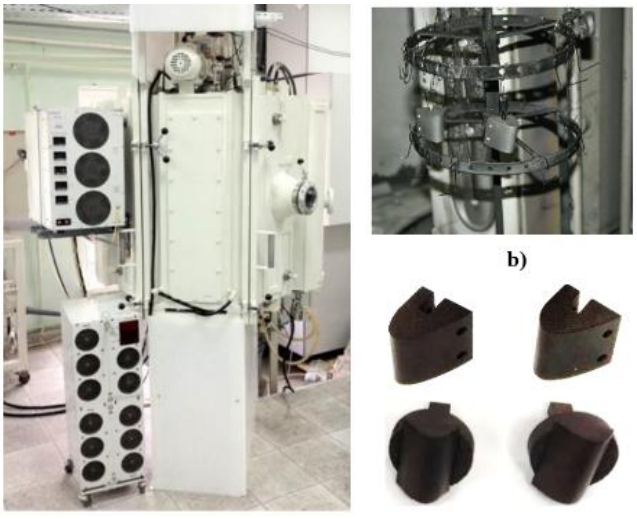

Fig. 5. External view of Gefest–HiPIMS facility (a), couplings and experimental samples before (b) and after (c) formation of DLC coating.

IV. STUDYING COATING PROPERTIES AND EROSION RESISTANCE

The coating microhardness was measured using a *DuraScan* 20 hardness meter in various points under the load of 0.05 kgf (0.49 N). The coating thickness was determined on transversal polished cross section using a *Tescan MIRA* 3 *LMU* scanning electron microscope. The images of polished sections were acquired in back reflection electrons giving contrast according to atomic number. Morphology of sample surface was also studied using electron microscope in secondary electrons providing information about surface relief. Elemental composition of coating was determined using a *GD Profiler*–2 optical emission glow discharge spectrometer as well as *X–Max* 50 X-ray energy dispersion spectrometer (*EDS*) *X–Max* 50, installed in a *Tescan MIRA* 3 *LMU* microscope. Surface roughness of samples was determined using a *Surftest SJ*–210 portable contact profile meter.

The experimental Ti–6Al–4V samples fabricated by 3D printing without and with DLC coating were tested using Erosion–M hydroimpact test rig, Moscow Power Engineering Institute (Fig. 6) [32].

The hydroimpact test rig is a facility of rotary type operating as follows: two considered samples are fixed at the edges of titanium alloy rod rotating in vacuum chamber and crossing vertical flow of droplets (Fig. 7) escaping from special droplet generator.

Fig. 6. Erosion–M hydroimpact test rig

The samples were tested in pairs, i.e. one test was carried out simultaneously with Ti–6Al–4V samples fabricated by 3D printing without and with DLC coating. The tests were performed at impingement velocity C_{imp} = 300 m/s with liquid droplets with the diameter d_{dr} = 800 μm. The time of sample tests was varied.

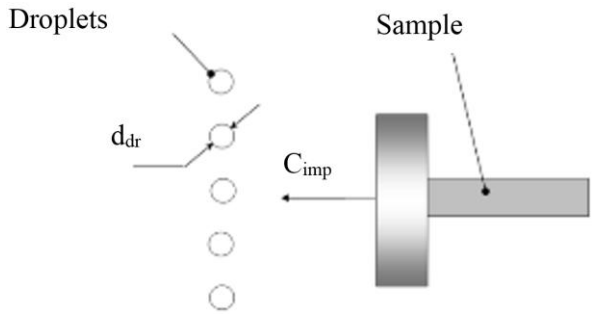

Fig. 7. Interaction of samples with liquid droplets: d_{dr} – droplet diameter; C_{imp} – sample velocity

Erosion curve was plotted using at least six different times of exposure. Erosion tests were compared on the basis of sample weight loss Δm, (g) as a function of time of exposure on the test rig t, (min) (Fig. 8), the experimental points were depicted. The relative error of Δm was δm = 5%. The sample weight loss was determined as follows:

$$\Delta m_i = m_0 - m_i,$$

where m_0 is the initial weight of sample; m_i is the weight of sample after test; i was the test number.

The main properties of erosion wear were determined and compared on the basis of the obtained kinetic curves. The duration of incubation period was determined as the segment between the coordinate origin and point of interception of tangent to the segment with maximum erosion rate with abscissa: time of exposure *t*, min (Fig. 8). The relative erosion resistance of Ti–6Al–4V samples fabricated by 3D printing with protective DLC coating was presented in the form of histograms where their duration of incubation period was compared with regard to similar value for Ti–6Al–4V samples fabricated by 3D printing without coating (reference), their values were assigned to unity.

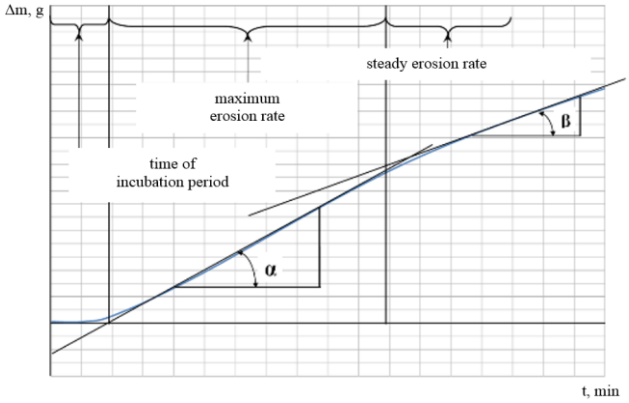

Fig. 8. Determination of main properties of erosion wear

V. RESULTS

Measured thickness, microhardness, and composition of coating formed on the surface of experimental samples and couplings are summarized in Table II.

Table II. Measured microhardness, thickness and composition of coatings

No.	Description	Composition	Coating thickness δ, μm	Microhardness HV 0.05
1	Sample with blade profile of *Ti*–6*Al*–4*V* with *DLC* coating	*DLC* layer: 67 wt % *C*, 17 wt % *O*, 16 wt. % *Ti*. *TiC* layer: 95 wt % *Ti*, 5 wt % *C*	3.6±0.2	820±50
2	*Ti*–6*Al*–4*V* coupling with *DLC* coating	*DLC* layer: 70 wt % *C*, 23 wt % *O*, 1 wt % *N*, 6 wt % *Ti*. *TiC* layer: 91 wt % *Ti*, 9 wt % *C*	3.4±0.2	890±60

The thickness of formed coating with upper *DLC* layer is about 3.4÷3.6 μm. The structure of coating surface is grained, the grain size varies in the range from 40 to 230 nm (Fig. 9).

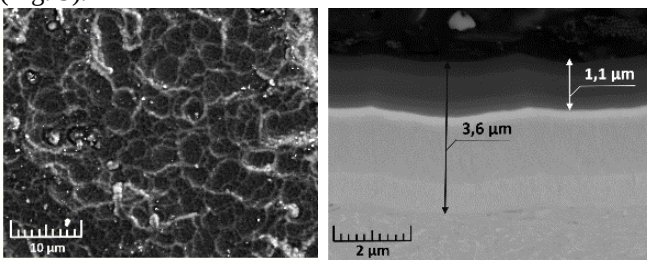

a) b)

Fig. 9. Morphology (a) and surface structure (b) of erosion resistant coupling with DLC coating

The *DLC* layer contains in average from 67 to 73% C, from 17 to 23% O, about 1% N, from 6 to 16% Ti. The content of titanium decreases towards surface accompanied by increase in oxygen content (Fig. 10).

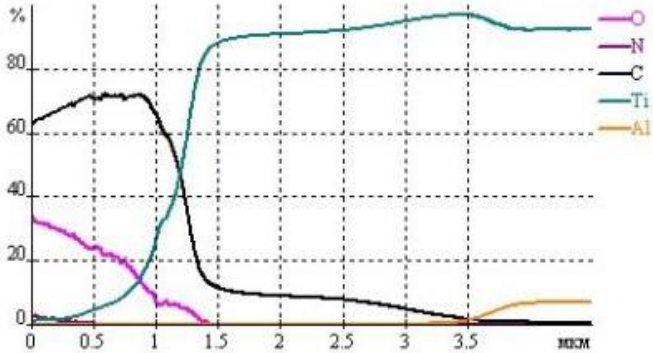

Fig. 10. Elemental composition as a function of depth of coating surface layer on *Ti*–6*Al*–4*V* coupling

The surface roughness (Ra) of *Ti*–6*Al*–4*V* samples with coating was 1.4 μm, and that of initial surface – 3.5 μm.

Kinetic erosion curves (Fig. 11a) were obtained after tests with Ti–6Al–4V samples fabricated by 3D printing without and with DLC coating at the impingement velocity of samples C_{imp} = 300 m/s with liquid droplets with the diameter of d_{dr} = 800 μm. Comparison of relative resistance with respect to duration of incubation period of material without and with coating is illustrated in the form of histogram in Fig. 11b.

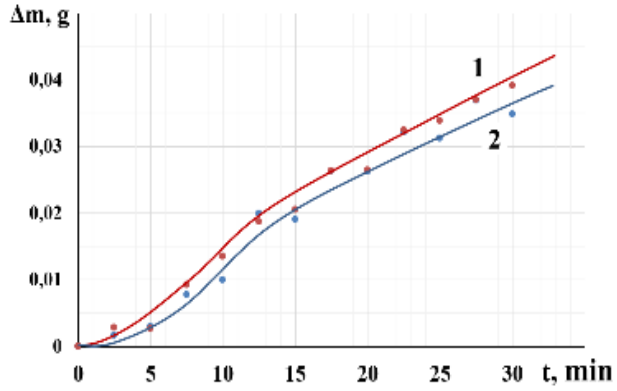

a)

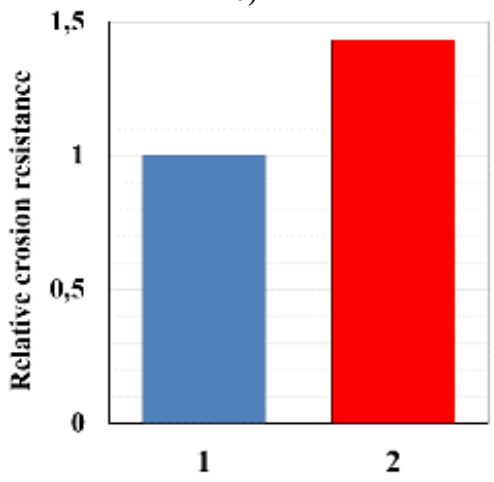

b)

Fig. 11. Tests of Ti–6Al–4V samples fabricated by 3D printing without (1) and with (2) DLC coating

VI. DISCUSSION

The external view of samples simulating leading edge of a coupling after 5 min tests as the view of destruction of material surface without coating and with DLC coating is illustrated in Fig. 12. The depicted fracture patterns of sample surface show that the upper layer of DLC coating is destroyed not uniformly along overall length and width of erosion trace in the form of separate flakes at its sides, leaving small areas of main materials in remote locations. Such defoliation can evidence insufficient adhesion of coating to titanium substrate upon high energy pulse impact of liquid droplets. Probably, protective properties of coating against droplet impingement are active only during incubation period with subsequent wear of main material. The formed variant of DLC coating increases duration of incubation period of water droplet impact erosion, and after removal of coating at the point of impact the substrate main material erosion rate remains unchanged during maximum and steady periods.

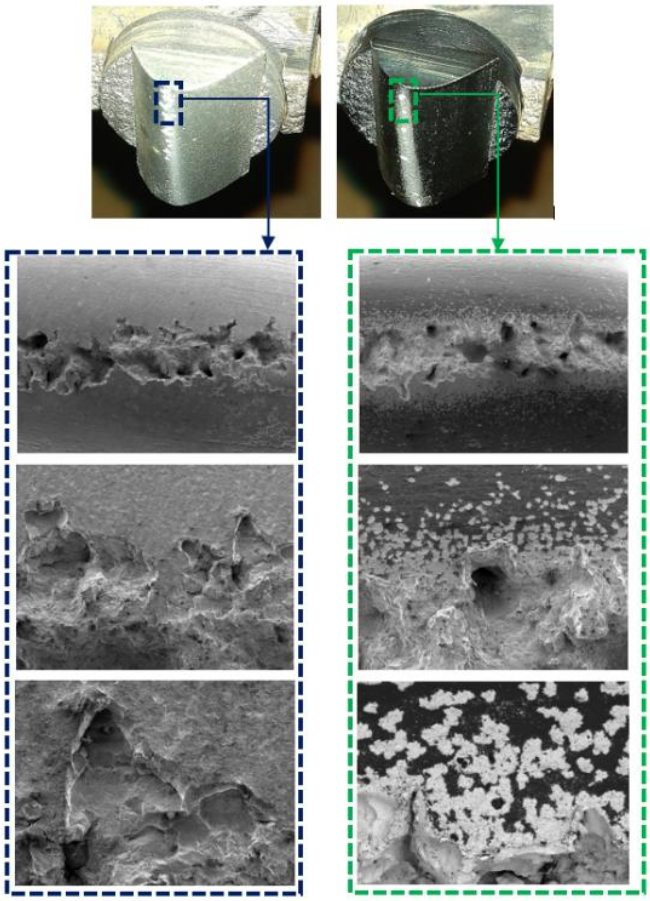

a) b)

Fig. 12. Fracture patterns of samples (various magnification) simulating leading edge of coupling without (a) and with (b) DLC coating

The variant implemented in full scale assuming replacement of worn couplings with new ones with and without coating (DLC coating in this case) is illustrated in Fig. 13.

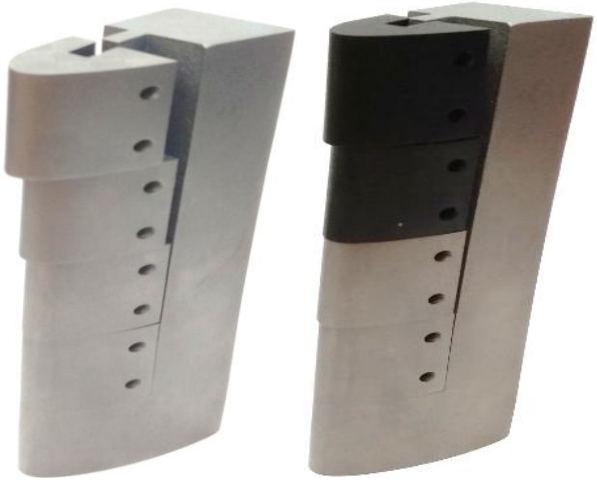

a) b)

Fig. 13. Blade part of the steam turbine last stage: a) variant with unreinforced couplings; b) variant with two erosion resistant couplings with protective DLC coating

Published By:
Blue Eyes Intelligence Engineering
& Sciences Publication

VII. CONCLUSION

1. As a consequence of experiments with workpieces simulating erosion resistant couplings at rotating blade periphery fabricated by 3D printing, the protective DLC coating was formed, its properties and resistance against water droplet impact erosion were studied.
2. The thickness of fabricated protective coatings based on DLC was from 3.3 to 4.1 μm. The DLC coatings contained up to 85–93 at % C, from 2 to 7 at % Ti, and from 1 to 10 at % O.
3. It has been established that the DLC coatings formed on printed workpieces of powdered titanium increase their erosion resistance in terms of time of incubation period by at least 1.4 times.
4. It has been demonstrated that 3D printing can be applied not only for production of serviceable replacement but also for fabrication of parts of titanium rotating blades exposed to water droplet impact erosion with their subsequent strengthening by formation of wear resistant coating including DLC coatings.

VIII. ACKNOWLEDGMENT

This work was supported by Russian Science Foundation, project No. 17–79–10462 dated August 01, 2017.

REFERENCES

1. S.N. Litunov, I.A. Sysuev, V.M. Vdovin, “Printing: technology, equipment, materials”. *Materials VI bypass. scientific–practical conf. from Intern. participation*. Omsk: Publishing House Omsk. state tech. University, 2015.
2. L.P. Babentsova and Antsiferova I.V. “Quality and ecology of selective laser sintering technology”. *Master`s Journal*, *vol. 1*, 2017, pp. 87–92.
3. V. Navrotsky, A. Graichen, and H. Brodin, Industrialization of 3D printing (additive manufacturing) for gas turbine components repair and manufacturing”. *VGB PowerTech*, *vol. 12*, 2015, pp. 48–52.
4. C. Zopp, S. Blümer, F. Schubert, and L. Kroll, “Processing of a metastable titanium alloy (Ti–5553) by selective laser melting Ain Shams”. *Engineering Journal*, *vol. 8*, 2017, pp. 475–9.
5. U.K. Mohanty, J. Rana, and A. Sharma, “Multi–objective optimization of electro–discharge machining (EDM) parameter for sustainable machining”. *Materials Today: Proceedings*, *vol. 4*, 2017, pp. 9147–57.
6. A. Dadgari, D. Huo, and D. Swailes, “Investigation on tool wear and tool life prediction in micro–milling of Ti–6Al–4V”. *Nanotechnology and Precision Engineering*, *vol. 1*, 2018, pp. 218–25
7. P. Sneha, A. Mahamani, and I. Kakaravada, “Optimization of wire electric discharge machining parameters in machining of Ti–6Al–4V alloy”. *Materials Today: Proceedings*, *vol. 5*, 2018, pp. 6722–6727.
8. V.S. Sufiiarova, A.A. Popovicha, E.V. Borisova, I.A. Polozova, D.V. Masayloa, and A.V. Orlov, “The effect of layer thickness at selective laser melting”. *Procedia Engineering*, *vol. 174*, 2017, pp. 126–34.
9. A.K. Rouniyar, and P. Shandilya, “Multi–objective optimization using Taguchi and Grey relational analysis on machining of Ti–6Al–4V alloy by powder mixed EDM process”. *Materials Today: Proceedings*, *vol. 5*, 2018, pp. 23779–88.
10. P. Edwards, and M. Ramulu, “Fatigue performance evaluation of selective laser melted Ti–6Al–4V”. *Materials Science & Engineering A*, *vol. 598*, 2014, pp. 327–337.
11. R. Konečná, L. Kunz, A. Bača, and G. Nicoletto, “Long fatigue crack growth in Ti6Al4V produced by direct metal laser sintering”. *Procedia Engineering*, *vol. 160*, 2016, pp. 69–76.
12. P. Chandramohan, B. Shepherd, B.A. Obadele, and P.A. Olubambi, “Laser additive manufactured Ti–6Al–4V alloy: tribology and corrosion studies”. *International Journal Adv Manuf Technol*, *vol. 92*, 2017, pp. 3051–61.
13. D. Zhao, Y. Huang, Y. Ao, C. Han, Q. Wang, Y. Li, J. Liu, Q. Wei, and Z. Zhang, “Effect of pore geometry on the fatigue properties and cell affinity of porous titanium scaffolds fabricated by selective laser melting”. *Journal of the Mechanical Behavior of Biomedical Materials*, *vol. 88*, 2018, pp. 478–487.
14. A.F. Mednikov, A.B. Tkhabisimov, A.A Makeeva, and M.R Dasaev, “Comparative erosion tests results of titanium alloy Ti–6Al–4V samples obtained by using 3D – Printing technology and manufactured by the traditional technological method”. Journal of Physics: Conference Series, vol. 1050(1), 2018.
15. RD 153–34.1–17.462–00. “Guidelines regarding the evaluation procedure of working capacity of steam turbine work blades during their manufacturing, operation and repairs”.
16. N.D. Prasanna, C. Siddaraju, G. Shetty, M.R. Ramesh, and M. Reddy, “Studies on the role of HVOF coatings to combat erosion in turbine alloys”. Materials Today: Proceedings, vol. 5, 2018, pp. 3130–6.
17. P. Wieciński, J. Smolik, H. Garbacz, and K.J. Kurzydłowski, “Erosion resistance of the nanostructured Cr/CrN multilayer coatings on Ti6Al4V alloy”. Vacuum, vol. 107, 2014, pp. 277–283.
18. R. Rajendran, “Gas turbine coatings – An overview”. Eng. Fail. Anal., vol. 26, 2012, pp. 355–62.
19. L. Swadzba, B. Formanek, H.M. Gabriel, P. Liberski, and P. Podolski, “Erosion– and corrosion–resistant coatings for aircraft compressor blades”. Surf. Coat. Technol., vol. 62, 1993, pp. 486–92.
20. A.F. Mednikov, V.A. Ryzhenkov, L.I. Seleznev, and A.I. Lebedeva, “Studying the variation of parameters characterizing the material surface during the droplet erosion incubation period”. Thermal Engineering, vol. 59(5), 2012, pp. 414–20.
21. E.F. Tchaikovsky, V.M. Puzikov, and A.V. Semenov, “Diamond–like carbon films”. Review. inf. sir "Single crystals and highly pure substances". Moscow: NIITEKHIM, 1985.
22. J. Robetson, “Dimond–like amorphous carbon”. Materials Science and engineering R, vol. 37, 2002, pp. 129–281.
23. Y. Lifshitz, “Diamond–like carbon – present status”. Diamond and Related Materials, vol. 8, 1999, pp. 1659–76.
24. D.R. McKenzie, “Tetrahedral bonding in amorphous carbon”. Rep. Prog. Phys, vol. 59, 1996, pp. 1611–64.
25. I.I. Aksenov, and V.E. Strel’nitskij, “Vacuum–arc discharge as an instrument for PVD process of DLC films deposition”. Diamond films and films of related materials: Sat. report 5th International Symposium. Kharkov: NSC KIPT, 2002, pp. 39–64.
26. P.H. Gaskell, “Neutron–scattering studies of the structure of highly tetrahedral amorphous diamond–like carbon”. Phys. Rev. Lett. vol. 67, 1991, pp. 1286–9.
27. V.P. Goncharenko, A.Y. Kolpakov, and A.I. Maslov, “The structure and properties of diamond–like carbon films, the mechanisms of their formation from the pulsed plasma flow”. Proceedings of the VII Conference of the CIS countries "Radiation damageability and performance of structural materials". Belgorod, 1997, pp. 146–8.
28. S.S. Olevsky, “Features of the structure and chemical composition of diamond–like carbon films”. Surface. Physics, chemistry, mechanics, vol. 7, 1982, pp. 118–25.
29. S.V. Hainsworth, N.J. Uhure, “Diamond–like carbon for tribology: production techniques, characterization methods and applications”. International Materials reviews, vol. 52, 2013, pp. 153–74.
30. Bolee Machine Tool. “M2 Cusing Metal 3D Printer”. [online]. Available: http://www.bolee.com.hk/m2-cusing-metal-3d-printer/
31. PADT. [online]. Available: http://www.padtinc.com/downloads/Webinar–3dmp–1.pdf
32. MPEI. [online]. Available: http://usu-erosion.mpei.ru/equipment/Pages/default.aspx